

Effects of Arctic stratospheric ozone changes on spring precipitation in the northwestern United States

Xuan Ma¹, Fei Xie^{1*}, Jianping Li^{1,2}, Xinlong Zheng¹, Wenshou Tian³,
Ruiqiang Ding⁴, Cheng Sun¹, and Jiankai Zhang³

¹*State Key Laboratory of Earth Surface Processes and Resource Ecology and College of Global Change and Earth System Science, Beijing Normal University, Beijing, China*

²*Laboratory for Regional Oceanography and Numerical Modeling, Qingdao National Laboratory for Marine Science and Technology, Qingdao, China*

³*College of Atmospheric Sciences, Lanzhou University, Lanzhou, China*

⁴*State Key Laboratory of Numerical Modeling for Atmospheric Sciences and Geophysical Fluid Dynamics, Institute of Atmospheric Physics, Chinese Academy of Sciences, Beijing, China*

Submitted as an Article to: *Atmospheric Chemistry and Physics*

13 September 2018

* Corresponding author:

Dr. Fei Xie, Email: xiefei@bnu.edu.cn.

1 **Abstract**

2 Using observations and reanalysis, we find that changes in April precipitation
3 variations in the northwestern US are strongly linked to March Arctic stratospheric
4 ozone (ASO). An increase in ASO can result in enhanced westerlies in the high and
5 low latitudes of the North Pacific but weakened westerlies in the mid-latitudes. The
6 anomalous circulation over the North Pacific can extend eastward to western North
7 America, facilitating the flow of a dry and cold airstream from the middle of North
8 America to the North Pacific and enhancing downwelling in the northwestern US,
9 which results in decreased precipitation there, and vice versa for the decrease in ASO.
10 Model simulations using WACCM4 support the statistical analysis of observations
11 and reanalysis data, and further reveal that the ASO influences circulation anomalies
12 over the northwestern US in two ways. Stratospheric circulation anomalies caused by
13 the ASO changes can propagate downward to the troposphere in the North Pacific and
14 then eastward to influence the strength of the circulation anomalies over the
15 northwestern US. In addition, sea surface temperature anomalies over the North
16 Pacific, which may be related to the ASO changes, would cooperate with the ASO
17 changes to modify the circulation anomalies over the northwestern US. Our results
18 suggest that ASO variations could be a useful predictor of spring precipitation
19 changes in the northwestern US.

20 **1. Introduction**

21 Stratospheric circulation anomalies can affect tropospheric climate via chemical–
22 radiative–dynamical feedback processes (Baldwin and Dunkerton, 2001; Graf and
23 Walter, 2005; Cagnazzo and Manzini, 2009; Ineson and Scaife, 2009; Thompson et al.,
24 2011; Reichler et al., 2012; Karpechko et al., 2014; Kidston et al., 2015; Li et al.,
25 2016; Zhang et al., 2016; Wang et al., 2017). Since stratospheric ozone can influence
26 stratospheric temperature and circulation via the atmospheric radiation balance (Tung,
27 1986; Haigh, 1994; Ramaswamy et al., 1996; Forster and Shine, 1997; Pawson and
28 Naujokat, 1999; Solomon, 1999; Randel and Wu, 1999, 2007; Labitzke and Naujokat,
29 2000; Gabriel et al. 2007; Gillett et al. 2009; McCormack et al. 2011), the impact of
30 ozone on tropospheric climate change has recently received widespread attention (e.g.,
31 Nowack et al. 2015, 2017, 2018).

32 In recent decades, Antarctic stratospheric ozone has decreased dramatically due
33 to the increase in anthropogenic emissions of ozone depleting substances (Solomon,
34 1990, 1999; Ravishankara et al., 1994, 2009). Numerous studies have found that the
35 decreased Antarctic ozone has contributed substantially to climate change in the
36 Southern Hemisphere. The Southern Hemisphere circulation underwent a marked
37 change during the late 20th century, with a slight poleward shift of the westerly jet
38 (Thompson and Solomon, 2002; Archer and Caldeira, 2008). The poleward
39 circulation shift would cause surface temperature anomalies by affecting localized
40 wind patterns and associated thermal advection (Son et al., 2010; Thompson et al.
41 2011; Feldstein, 2011). Subsequent studies concluded that Antarctic ozone depletion
42 is responsible for at least 50% of the circulation shift (Lu et al., 2009; Son et al., 2010;
43 McLandress et al., 2011; Polvani et al., 2011; Hu et al., 2013; Gerber and Son, 2014;
44 Waugh et al., 2015). In addition, the poleward displacement of the westerly jet has

45 been linked to an extension of the Hadley cell (Son et al., 2009, 2010; Min and Son,
46 2013) and variations in mid- to high-latitude precipitation during austral summer; i.e.,
47 increased rainfall in the subtropics and high latitudes and reduced rainfall in the
48 mid-latitudes of the Southern Hemisphere (Son et al., 2009; Feldstein, 2011; Kang et
49 al., 2011; Polvani et al., 2011). The changes in Antarctic ozone are not only related to
50 the displacement of the westerly jet in the Southern Hemisphere, but also affect its
51 intensity. Thompson and Solomon (2002) argued that Antarctic ozone depletion can
52 also enhance westerly winds via the strong radiative cooling effect and thermal wind
53 relationship. The westerly winds are enhanced from the stratosphere to the
54 mid-latitude troposphere in the case of wave–mean flow interaction (Son et al., 2010;
55 Thompson et al., 2011), thereby accelerating circumpolar currents in the mid-latitudes.
56 Moreover, changes in subtropical drought, storm tracks and ocean circulation in the
57 Southern Hemisphere are also closely related to Antarctic ozone variations (Yin, 2005;
58 Russell et al., 2006; Son et al., 2009; Polvani et al., 2011; Bitz and Polvani, 2012).

59 The variations in Arctic stratospheric ozone (ASO) in the past five decades are
60 quite different from those of Antarctic stratospheric ozone, as the multi-decadal loss
61 of ASO is much smaller than that of Antarctic stratospheric ozone (WMO, 2011).
62 However, sudden stratospheric warming in the Arctic (Randel, 1988; Charlton and
63 Polvani, 2007; Manney et al., 2011; Manney and Lawrence, 2016) means that the
64 year-to-year variability in ASO has an amplitude equal to or even larger than that of
65 Antarctic stratospheric ozone. Thus, the effect of ASO on Northern Hemisphere
66 climate change has also become a matter of concern.

67 Comparing with the effect of the winter stratospheric dynamical processes on the
68 tropospheric North Atlantic Oscillation (NAO) and the incidence of extreme weather

69 events (Baldwin and Dunkerton, 2001; Black et al., 2005, 2006, 2009), the depletion
70 of spring ASO can cause circulation anomalies that influence the North Pacific
71 Oscillation. Cheung et al. (2014) used the UK Met Office operational weather
72 forecasting system and Karpechko et al. (2014) used ECHAM5 simulations to
73 investigate the relationship between extreme Arctic ozone anomalies in 2011 and
74 tropospheric climate. Smith and Polvani (2014) used an atmospheric global climate
75 model to reveal a significant influence of ASO changes on tropospheric circulation,
76 surface temperature, and precipitation when the amplitudes of the forcing ASO
77 anomaly in the model are larger than those historically observed. Subsequently, using
78 a fully coupled chemistry–climate model, Calvo et al. (2015) again confirmed that
79 changes in ASO can produce robust anomalies in Northern Hemisphere temperature,
80 wind, and precipitation. Furthermore, the effects of ASO on the Northern Hemisphere
81 climate can be seen in observations. Ivy et al. (2017) presented observational evidence
82 for the relationship between ASO and tropospheric climate, revealing that the
83 maximum daily surface temperature anomalies in spring (March–April) in some
84 regions of the Northern Hemisphere occurred during years with low ASO in March.
85 Xie et al. (2016, 2017a, 2017b) demonstrated that the tropical climate can also be
86 affected by ASO. They pointed out that stratospheric circulation anomalies caused by
87 March ASO changes can rapidly extend to the lower troposphere and then propagate
88 horizontally to the North Pacific in about 1 month, influencing the North Pacific sea
89 surface temperature (SST) in April. The induced SST anomalies (Victoria Mode)
90 associated with the circulation anomalies can influence El Niño–Southern Oscillation
91 (ENSO) and tropical rainfall over a timescale of ~20 months.

92 As shown above, a large number of observations and simulations have shown
93 that ASO variations have a significant impact on Northern Hemisphere tropospheric

94 climate, but few studies have focused on regional characteristics. Xie et al. (2018)
95 found that the ASO variations could significantly influence rainfall in the central
96 China, since the circulation anomalies over the North Pacific caused by ASO
97 variations can extend westward to China. This motivates us to investigate whether the
98 circulation anomalies extend eastward to affect the precipitation in North America. In
99 this study, we find a strong link between ASO and precipitation in the northwestern
100 US in spring. We focus on analyzing the characteristics of the impact of ASO on
101 precipitation in the northwestern US in spring and the associated mechanisms. The
102 remainder of this manuscript is organized as follows. Section 2 describes the data and
103 numerical simulations, and section 3 discusses the relationship between the ASO
104 anomalies and precipitation variations in the northwestern US, as well as the
105 underlying mechanisms. The results of simulations are presented in section 4, and
106 conclusions are given in section 5.

107 **2. Data and simulations**

108 The ASO variations is defined as the Arctic stratospheric ozone averaged over the
109 latitude of 60° – 90° N at an altitude of 100–50 hPa after removing the seasonal cycle
110 and trend. Ozone values used in the present analysis are derived from the
111 Stratospheric Water and OzOne Satellite Homogenized (SWOOSH) dataset (Davis et
112 al., 2016), which is a collection of stratospheric ozone and water vapor measurements
113 obtained by multiple limb sounding and solar occultation satellites over the previous
114 30 years. Monthly mean ozone data from SWOOSH (1984–2016) is zonal–mean
115 gridded dataset at a horizontal resolution of 2.5° (latitude: 89° S to 89° N) and vertical
116 pressure range of 31 levels from 316 hPa to 1 hPa. Another set of ozone data is taken
117 from Global Ozone Chemistry and Related trace gas Data Records for the
118 Stratosphere (GOZCARDS, 1984–2013) project (Froidevaux et al., 2015) based on

119 high quality data from past missions (e.g., SAGE, HALOE data) and ongoing
120 missions (ACE-FTS and Aura MLS). It is also a zonal–mean dataset with a
121 meridional resolution of 10° , extending from the surface to 0.1 hPa (25 levels).

122 In addition, two sets of global precipitation reanalysis datasets are employed in
123 this study: monthly mean precipitation data constructed by the Global Precipitation
124 Climatology Project (GPCP), which is established by the World Climate Research
125 program (WCRP) in 1986 aiming to observe and estimate the spatial and temporal
126 global precipitation (Huffman et al., 1997), with a resolution of 2.5° latitude/longitude
127 grid for the analysis period 1984–2016; global terrestrial rainfall dataset derived from
128 the Global Precipitation Climatology Centre (GPCC) based on quality-controlled data
129 from 67200 stations world-wide, with a resolution of 1.0° latitude/longitude grid. In
130 addition, SST is taken from the UK Met Office Hadley Centre for Climate Prediction
131 and Research SST (HadSST). Other atmospheric datasets including monthly-mean
132 wind and geopotential height fields for the period 1984–2016 are obtained from the
133 NCEP/Department of Energy (DOE) Reanalysis 2 (NCEP-2), regarded as an updated
134 NCEP/NCAR Reanalysis Project (NCEP-1).

135 We use the Whole Atmosphere Community Climate Model version 4
136 (WACCM4), a part of the National Center for Atmospheric Research’s Community
137 Earth System Model (CESM), version 1.0.6, to investigate precipitation response in
138 the northwestern United States to the ASO anomalies. WACCM4 encompasses the
139 Community Atmospheric Model version 4 (CAM4) and as such includes all of its
140 physical parameterizations (Neale et al., 2013). It uses a system made up of four
141 components, namely atmosphere, ocean (specified SST), land, and sea ice (Holland et
142 al., 2012) and has detailed middle–atmosphere chemistry. This improved version of

143 WACCM uses a finite-volume dynamical core, and it extends from the surface to
144 approximately 145 km geometric altitude (66 levels), with a vertical resolution of
145 about 1 km in the tropical tropopause layer and the lower stratosphere. Note that the
146 simulations in the present paper are disable interactive chemistry as WACCM4-GHG
147 scheme (Garcia et al., 2007) with a $1.9^\circ \times 2.5^\circ$ horizontal resolution. More
148 information can be seen in Marsh et al. (2013). The model's radiation scheme uses
149 these conditions: fixed greenhouse gas (GHG) values (averages of emissions scenario
150 A2 of the Intergovernmental Panel on Climate Change (WMO, 2003) over the period
151 1995–2005). The prescribed ozone forcing used in the experiments is a 12–month
152 seasonal cycle averaged over the period 1995–2005 from CMIP5 ensemble mean
153 ozone output. The Quasi Biennial Oscillation (QBO) phase signals with a 28–month
154 fixed cycle are included in WACCM4 as an external forcing for zonal wind.

155 Seven time–slice experiments (R1–R7) are designed to investigate the
156 precipitation changes in the northwestern US due to the ASO anomalies. Details of the
157 seven experiments are given in Table 1. All the experiments are run for 33 years, with
158 the first 3 years excluded for the model spin–up and only the last 30 years are used for
159 analysis.

160 **3. Response of precipitation in the northwestern US to ASO anomalies in** 161 **spring**

162 Since the variations in ASO are most obvious in March due to the Arctic polar vortex
163 break down (Manney et al., 2011), previous studies have reported that the ASO
164 changes in March have the strongest influence on the Northern Hemisphere (Ivy et al.,
165 2017; Xie et al., 2017a). In addition, these studies pointed out that the changes in ASO
166 affect the tropospheric climate with a lead of about 1–2 months, which is similar to

167 the troposphere response to the Northern Hemisphere sudden stratospheric warmings
168 (Baldwin and Dunkerton 2001; Black et al., 2005, 2006, 2009) and Southern
169 Hemisphere stratospheric ozone depletion (Thompson and Solomon 2002); the
170 relevant mechanisms have been investigated in detail by Xie et al. (2017a). We
171 therefore show in Fig. 1 the correlation coefficients between ASO variations in March
172 from SWOOSH and GOZCARDS data, and precipitation anomalies in April from
173 GPCP and GPCP data over western North America. In all cases in Fig. 1 the March
174 ASO changes are significantly anti-correlated with April precipitation anomalies in
175 the northwestern US (mainly in Washington and Oregon), implying that positive
176 spring ASO anomalies are associated with less spring precipitation in the
177 northwestern US, and vice versa for the negative spring ASO anomalies. Note that
178 since this kind of feature appears in the northwestern US, Fig. 1 shows only the west
179 side of North America.

180 The correlation coefficients between March ASO variations and precipitation
181 anomalies (January to December are in the same year) in the northwestern US are
182 shown in Fig. 2. The correlation coefficients between March ASO variations and April
183 precipitation anomalies in the northwestern US are the largest and are significant at
184 the 95% confidence level. Note that the correlation coefficients between March ASO
185 variations and July precipitation anomalies are also significant. The impact of March
186 ASO on precipitation in the northwestern US in summer and the associated
187 mechanisms are different from those considered in this study (not shown) and will be
188 presented in another paper, but will not be investigated further here. March ASO
189 changes are not significantly correlated with simultaneous (March) precipitation
190 variations (Fig. 2), illustrating that the ASO changes lead precipitation anomalies by
191 about 1 month. Since the results from four sets of observations show a common

192 feature, and SWOOSH and GPCP data span a longer period, only SWOOSH ozone
193 and GPCP precipitation are used in the following analysis.

194 The above statistical analysis shows a strong negative correlation between March
195 ASO variations and April precipitation anomalies in the northwestern US, meaning
196 that the ASO can be used to predict changes in spring precipitation in the
197 northwestern US. The process and underlying mechanism that are responsible for the
198 impact of ASO anomalies on precipitation changes need further analysis.

199 Figure 3 shows the correlation coefficients between March ASO anomalies and
200 April zonal wind variations at 200, 500, and 850 hPa, respectively. The spatial
201 distribution of significant correlation coefficients over the North Pacific exhibits a
202 tripolar mode with a zonal distribution at 200 and 500 hPa; i.e. a positive correlation
203 in the high and low latitudes in the North Pacific and a negative correlation in
204 mid-latitudes. This implies that the increase in ASO can result in enhanced westerlies
205 in the high and low latitudes of the North Pacific but weakened westerlies in the
206 mid-latitudes, corresponding to the weakened Aleutian Low in April, and vice versa
207 for the decrease in ASO. The Aleutian Low acts as a bridge connecting variations in
208 ASO and circulation anomalies over the North Pacific (Xie et al., 2017a). At 850 hPa,
209 the anomalous circulation signal in the low latitudes of the North Pacific has
210 weakened and disappeared. It is evident that the anomalous changes in the zonal wind
211 over the North Pacific can extend westward to East Asia. Xie et al. (2018) identified
212 the effect of spring ASO changes on spring precipitation in China. Note that the
213 weakened westerlies in the mid-latitudes and the enhanced westerlies at low latitudes
214 can also extend eastward to the western United States. This kind of circulation
215 anomaly corresponds to two barotropic structures; i.e., an anomalous anticyclone in

216 the Northeast Pacific and a cyclone in the southwestern United States at 500 hPa and
217 200 hPa. Coincidentally, the northwestern United States is located to the north of the
218 intersection of the anticyclone and cyclone, corresponding to convergence of the
219 airflow at high levels, which may lead to downwelling in the northwestern United
220 States, and vice versa for negative March ASO anomalies.

221 To further validate our inference regarding the response of the circulation in the
222 western United States to ASO changes, we analyze the differences between April
223 horizontal wind anomalies during positive and negative March ASO anomaly events
224 at 200, 500, and 850 hPa (Fig. 4). As in the increased ASO case, the difference shows
225 an anomalous anticyclone in the Northeast Pacific and an anomalous cyclone in the
226 southwestern United States. This kind of circulation anomaly over the southwestern
227 United States enhances cold and dry airflow from the North American continent to the
228 North Pacific, reducing the water vapor concentration in the air over the western
229 United States and possibly reducing April precipitation in the northwestern United
230 States. In addition, the northwestern United States is located to the north of the
231 intersection of the anticyclone and cyclone, suggesting downwelling flow in the
232 region.

233 Figure 5a shows a longitude–latitude cross-section of differences in April vertical
234 velocity anomalies averaged over 1000–500 hPa between positive and negative March
235 ASO anomaly events. When the March ASO increases, anomalous downwelling is
236 found in the northwestern United States (115° – 130° W). This situation may inhibit
237 precipitation in the northwestern United States in April. Figure 5b depicts the
238 longitude–height cross-section of differences in April vertical velocity averaged over
239 43° – 50° N between positive and negative March ASO anomaly events, which further

240 shows an anomalous downwelling over the United States when the ASO increases.
241 Based on the above analysis, the circulation anomalies in the northwestern United
242 States associated with positive March ASO anomalies may inhibit the formation of
243 local precipitation in April, and vice versa for that with negative March ASO
244 anomalies.

245 **4. Simulations of the effect of ASO variations on precipitation in the** 246 **northwestern US during spring**

247 Using observations and reanalysis data, we investigated the relationship between
248 March ASO and April precipitation in the northwestern US and revealed the
249 underlying mechanisms in section 3. In this section, we use WACCM4 simulations
250 (see section 2) to confirm the above conclusions. First, we check the model
251 performance in simulating precipitation over western North America. Figure 6 shows
252 the April precipitation climatology over the region 95° – 140° W, 30° – 63° N from the
253 control experiment R1 (Table 1) and from GPCP for the period 1995–2005. The
254 model simulates a center of high precipitation over the west coast of North America
255 (Fig. 6a). It is clear that the spatial distribution of the simulated precipitation
256 climatology is similar to that calculated by GPCP (Fig. 6b).

257 Figure 7a displays the differences in April precipitation between experiments R3
258 and R2. The pattern of simulated April precipitation anomalies forced by ASO
259 changes in western North America (Fig. 7a) is different from that observed (Fig. 1);
260 i.e., the increased March ASO forces an increase in precipitation in the northwestern
261 United States. The differences in April zonal wind at 200, 500, and 850 hPa between
262 experiments R3 and R2 are shown in Fig. 7b, c, and d, respectively. The simulated
263 pattern of April zonal wind anomalies in western North America (Fig. 7b, c and d)

264 shifted a little further to the north than in the observations (Fig. 3). Comparing the
265 global pattern of simulated April zonal wind anomalies with the observations, it is
266 surprising to find that the positions of simulated zonal wind anomalies over the
267 Northeast Pacific and western North America are shifted northward. This results in
268 the simulated precipitation anomalies over western North America also shifting
269 northward, so that a decrease in precipitation on the west coast of Canada in April is
270 found in Fig. 7a. This explains why we find the pattern of simulated April
271 precipitation anomalies in the northwestern United States (Fig. 7a) is nearly opposite
272 to that observed (Fig. 1). Figure 7 shows that the results of the model simulation in
273 which we only change the ASO forcing do not reflect the real situation of April
274 precipitation anomalies in the northwestern United States, with a shift in position
275 compared with observations. This leads us to consider whether other factors interact
276 with March ozone to influence April precipitation in the northwestern United States.

277 Previous studies have found that the North Pacific SST has a significant effect on
278 precipitation in the United States (e.g., Namias, 1983; Ting and Wang, 1997; Wang
279 and Ting, 2000; Barlow et al., 2001; Lau et al., 2002; Wang et al., 2014). Figure 8a
280 shows the correlation coefficients between regional averaged (43° – 50° N, 115° –
281 130° W) precipitation anomalies and SST variations in April. Interestingly, the results
282 show that the distribution of correlation coefficients over the North Pacific has a
283 meridional tripole structure, which is referred to as the Victoria Mode SST anomaly
284 pattern. Xie et al. (2017a) demonstrated that the ASO has a lagged impact on the sea
285 surface temperature in the North Pacific mid–high latitudes based on observation and
286 simulation. They showed that stratospheric circulation anomalies caused by ASO
287 changes can rapidly extend to the lower troposphere in the high latitudes of the
288 Northern Hemisphere. The circulation anomalies in the high latitudes of the lower

289 troposphere take about a month to propagate to the North Pacific mid-latitudes and
290 then influence the North Pacific SST. Figure 8b shows the correlation coefficients
291 between March ASO (multiplied by -1) and April SST variations. The pattern in Fig.
292 8b is in good agreement with that in Fig. 8a. It is further found that removing the
293 Victoria Mode signal from the time series of precipitation in the northwestern United
294 States reduces the correlation coefficient between March ASO anomalies and filtered
295 April precipitation variations in the northwestern United States to -0.40 (the
296 correlation coefficient is -0.63 for the original time series, see Fig. 2), but it remains
297 significant. Figure 8 indicates that the ASO possibly influences precipitation
298 anomalies in the northwestern United States in two ways. First, the stratospheric
299 circulation anomalies caused by the ASO changes can propagate downward to the
300 North Pacific troposphere and eastward to influence precipitation over northwestern
301 United States. Second, the ASO changes generate SST anomalies over the North
302 Pacific that act as a bridge for ASO to affect precipitation in the northwestern United
303 States. The SST anomalies caused by ASO change likely interact with the direct
304 changes in atmospheric circulation driven by the ASO change to jointly influence
305 precipitation in the northwestern United States. Experiments R2 and R3 do not
306 include the effects of SST, which may explain why the results of the model simulation
307 in which we only change the ASO forcing do not reflect the observed precipitation
308 anomalies in the northwestern United States (Fig. 7).

309 Two sets of experiments (R4 and R5) that include the joint effects of ASO and
310 SST change (Fig. 9) are added. Details of the experiments are given in Table 1. Figure
311 10 shows the differences in April precipitation and zonal wind between experiments
312 R5 and R4. It is clear that the simulated changes in precipitation in the northwestern
313 United States (Fig. 10a) are in good agreement with the observed anomalies shown in

314 Fig. 1; i.e., the increase in March ASO forces a decrease in April precipitation in the
315 northwestern United States. In addition, the spatial distributions of simulated zonal
316 wind anomalies (Fig. 10b–d) are consistent with the observations (Fig. 3). Overall, the
317 simulated precipitation and circulation in R4 and R5 are no longer shifted northward
318 and are closer to the observations.

319 To further emphasize the importance of the joint effects of ASO and ASO-related
320 SST anomalies on precipitation in the northwestern United States, we investigate
321 whether the spring Victoria Mode-like SST anomalies alone could force the observed
322 precipitation anomalies in the northwestern United States. Two sets of experiments
323 are performed here (R6 and R7), in which only April SST anomalies over the North
324 Pacific have been changed (Fig. 9). Details of the experiments are given in Table 1.
325 Figure 11 shows the differences in April precipitation and zonal wind between
326 experiments R7 and R6. The simulated precipitation anomalies over the west coast of
327 the United States (Fig. 11a) are much weaker, and the simulated circulation
328 anomalies (Fig. 11b–d) are quite different from those in Fig. 3. This suggests that the
329 ASO-related North Pacific SST anomalies alone cannot force the observed
330 precipitation anomalies in the northwestern United States, but that the combined
331 effect of ASO and ASO-related North Pacific SST anomalies is required (Fig. 10).
332 Thus, we have shown that the relationship between March ASO and April
333 precipitation in the northwestern US in the observations and the underlying
334 mechanisms can be verified by WACCM4.

335 **5. Discussion and summary**

336 Many observations and simulations have shown that ASO variations have a
337 significant impact on Northern Hemisphere tropospheric climate, but few studies have

338 focused on regional characteristics. Using observations, reanalysis datasets, and
339 WACCM4, we have shown that spring ASO changes have a significant effect on April
340 precipitation in the northwestern United States (mainly in Washington and Oregon)
341 with a lead of 1–2 months. When the March ASO is anomalously high, April
342 precipitation decreases in the northwestern United States, and vice versa for low ASO.

343 During positive ASO events, the zonal wind changes over the North Pacific
344 exhibit a tripolar mode with a zonal distribution; i.e., enhanced westerlies in the high
345 and low latitudes of the North Pacific, and weakened westerlies in the mid-latitudes.
346 The anomalous wind can extend eastward to North America, causing anomalous
347 circulation in western North America. Such circulation anomalies force an anomalous
348 cyclone in the western United States in the middle and upper troposphere, which
349 likely enhances cold and dry airflow from the North American continent to the North
350 Pacific, reducing the water vapor concentration in the air over the northwestern
351 United States. At the same time, downwelling in the northwestern US is enhanced.
352 The two processes possibly decrease April precipitation in the northwestern US.
353 When the March ASO decreases, the effect is just the opposite.

354 The WACCM4 model is used to confirm the statistical results of observations
355 and the reanalysis data. The results of the model simulation in which we only change
356 the ASO forcing do not reflect the observed precipitation anomalies in the
357 northwestern United States in April; i.e., the pattern of simulated April precipitation
358 and circulation anomalies in the western North America shifted a little further to the
359 north than observed. It is found that SST anomalies over North Pacific caused by
360 ASO changes are likely to interact with ASO changes to jointly influence
361 precipitation in the northwestern United States. Thus, the ASO influences

362 precipitation anomalies over the northwestern United States in two ways. First, the
363 stratospheric circulation anomalies caused by the ASO change can propagate
364 downward to the North Pacific troposphere and directly influence precipitation over
365 the northwestern United States. Second, the ASO changes generate SST anomalies
366 over the North Pacific that act as a bridge, allowing the ASO changes to affect
367 precipitation in the northwestern United States.

368 It is well known that the spring ASO variations are related to changes in the
369 winter Arctic stratospheric vortex (SPV). The strength of the SPV can affect ASO,
370 and then ASO affects tropospheric teleconnection and precipitation in the
371 northwestern United States (indirect effect of SPV). The strength of the SPV may also
372 have a direct leading effect on tropospheric teleconnection (Baldwin and Dunkerton,
373 2001; Black et al., 2005, 2006, 2009) and precipitation in the northwestern United
374 States. Figure 12 shows the correlation coefficients between the February SPV
375 (multiplied by -1) index and April 200 hPa zonal wind and precipitation variations
376 (Fig. 12a and b), and between March ASO and April 200 hPa zonal wind and
377 precipitation (Fig. 12c and d). The SPV index is defined as the strength of the
378 stratospheric polar vortex, following Zhang et al. (2018). Although they are similar,
379 the ASO variations are much closer than the strength of the stratospheric polar vortex
380 to the variations in 200 hPa zonal wind and precipitation. That indicates indirect and
381 direct effects of winter SPV on spring tropospheric climate. Since the coupling
382 between dynamical and radiative processes in spring is strong, the connection
383 between winter SPV and spring tropospheric circulation seems weaker than that

384 between the spring ASO and tropospheric circulation. In this study, we try to state that
385 the ASO changes could influence precipitation in the northwestern United States,
386 emphasizing the influence of stratospheric ozone on tropospheric regional climate. As
387 for the effect of coupling between dynamical and radiative processes in spring on
388 precipitation is an interesting question that deserves further investigation.

389 **Acknowledgments.** Funding for this project was provided by the National Natural
390 Science Foundation of China (41630421, 41790474 and 41575039). We acknowledge
391 ozone datasets from the SWOOSH and GOZCARDS; precipitation from China
392 Meteorological Administration, GPCC and GPCP; Meteorological fields from NCEP2,
393 SST from the UK Met Office Hadley Centre, and WACCM4 from NCAR.

394 **References:**

- 395 Archer, C. L. and Caldeira, K.: Historical trends in the jet streams, *Geophys. Res.*
396 *Lett.*, 35, L08803, doi:10.1029/2008GL033614, 2008.
- 397 Baldwin, M. P. and Dunkerton, T. J.: Stratospheric harbingers of anomalous weather
398 regimes, *Science*, 294, 581–584, doi:10.1126/science.1063315, 2001.
- 399 Barlow, M., Nigam, S., and Berbery, E. H.: ENSO, Pacific decadal variability, and US
400 summertime precipitation, drought, and stream flow, *J. Climate*, 14, 2105–2128,
401 doi:10.1175/1520-0442(2001)014<2105:EPDVAU>2.0.CO;2, 2001.
- 402 Bitz, C. M. and Polvani, L. M.: Antarctic climate response to stratospheric ozone
403 depletion in a fine resolution ocean climate model, *Geophys. Res. Lett.*, 39,
404 L20705, doi:10.1029/2012GL053393, 2012.
- 405 Black, R. X., Mcdaniel, B. A., and Robinson, W. A.: Stratosphere Troposphere
406 Coupling during Spring Onset, *J. Climate*, 19, 4891–4901,
407 doi:10.1175/Jcli3907.1, 2005.
- 408 Black, R. X., and Mcdaniel, B. A.: The Dynamics of Northern Hemisphere
409 Stratospheric Final Warming Events, *J. Atmos. Sci.*, 64, 2932–2946,
410 doi:10.1175/Jas3981.1, 2006.
- 411 Black, R. X. and Mcdaniel, B. A.: SubMonthly polar vortex variability and
412 stratosphere-troposphere coupling in the Arctic, *J. Climate*, 22, 5886–5901,
413 doi:10.1175/2009JCLI2730.1, 2009.
- 414 Cagnazzo, C. and Manzini, E.: Impact of the Stratosphere on the Winter Tropospheric
415 Teleconnections between ENSO and the North Atlantic and European Region, *J.*

416 Climate, 22, 1223–1238, doi:10.1175/2008JCLI2549.1, 2009.

417 Calvo, N., Polvani, L. M., and Solomon, S.: On the surface impact of Arctic
418 stratospheric ozone extremes, *Environ. Res. Lett.*, 10, 094003,
419 doi:10.1088/1748-9326/10/9/094003, 2015.

420 Charlton, A. J. and Polvani, L. M.: A new look at stratospheric sudden warmings. Part
421 I: Climatology and modeling benchmarks, *J. Climate*, 20, 449–469,
422 doi:10.1175/JCLI3996.1, 2007.

423 Cheung, J. C. H., Haigh, J. D., and Jackson, D. R.: Impact of EOS MLS ozone data on
424 medium-extended range ensemble weather forecasts, *J. Geophys. Res.*, 119,
425 9253–9266, doi:10.1002/2014JD021823, 2014.

426 Davis, S. M., Rosenlof, K. H., Hassler, B., Hurst, D. F., Read, W. G., Vomel, H.,
427 Selkirk, H., Fujiwara, M., and Damadeo, R.: The Stratospheric Water and
428 Ozone Satellite Homogenized (SWOOSH) database: a long-term database for
429 climate studies, *Earth Syst Sci Data*, 8, 461–490, doi:10.5194/essd-8-461-2016,
430 2016.

431 Feldstein, S. B.: Subtropical Rainfall and the Antarctic Ozone Hole, *Science*, 332,
432 925–926, doi:10.1126/science.1206834, 2011.

433 Forster, P. M. D. and Shine, K. P.: Radiative forcing and temperature trends from
434 stratospheric ozone changes, *J. Geophys. Res.*, 102, 10841–10855,
435 doi:10.1029/96JD03510, 1997.

436 Froidevaux, L., Anderson, J., Wang, H.-J., Fuller, R. A., Schwartz, M. J., Santee, M.
437 L., Livesey, N. J., Pumphrey, H. C., Bernath, P. F., Russell III, J. M., and

438 McCormick, M. P.: Global Ozone Chemistry And Related trace gas Data records
439 for the Stratosphere (GOZCARDS): methodology and sample results with a
440 focus on HCl, H₂O, and O₃, *Atmos. Chem. Phys.*, 15, 10471–10507,
441 doi:10.5194/acp-15-10471-2015, 2015.

442 Gabriel, A., Peters, D., Kirchner, I., and Graf, H. F.: Effect of zonally asymmetric
443 ozone on stratospheric temperature and planetary wave propagation, *Geophys.*
444 *Res. Lett.*, 34, L06807, doi:10.1029/2006GL028998, 2007.

445 Garcia, R. R., Marsh, D. R., Kinnison, D. E., Boville, B. A., and Sassi, F.: Simulation
446 of secular trends in the middle atmosphere, 1950–2003, *J. Geophys. Res.*, 112,
447 D09301, doi:10.1029/2006JD007485, 2007.

448 Gerber, E. P. and Son, S. W.: Quantifying the Summertime Response of the Austral Jet
449 Stream and Hadley Cell to Stratospheric Ozone and Greenhouse Gases, *J.*
450 *Climate*, 27, 5538–5559, doi:10.1175/JCLI-D-13-00539.1, 2014.

451 Gillett, N. P., Scinocca, J. F., Plummer, D. A., and Reader, M. C.: Sensitivity of
452 climate to dynamically-consistent zonal asymmetries in ozone, *Geophys. Res.*
453 *Lett.*, 36, L10809, doi:10.1029/2009GL037246, 2009.

454 Graf, H. F. and Walter, K.: Polar vortex controls coupling of North Atlantic Ocean and
455 atmosphere, *Geophys. Res. Lett.*, 32, L01704, doi:10.1029/2004GL020664,
456 2005.

457 Haigh, J. D.: The Role of Stratospheric Ozone in Modulating the Solar Radiative
458 Forcing of Climate, *Nature*, 370, 544–546, doi:10.1038/370544a0, 1994.

459 Holland, M. M., Bailey, D. A., Briegleb, B. P., Light, B., and Hunke, E.: Improved

460 Sea Ice Shortwave Radiation Physics in CCSM4: The Impact of Melt Ponds and
461 Aerosols on Arctic Sea Ice, *J. Climate*, 25, 1413–1430,
462 doi:10.1175/JCLI-D-11-00078.1, 2012.

463 Hu, Y., Tao, L., and Liu, J.: Poleward expansion of the Hadley circulation in CMIP5
464 simulations, *Adv. Atmos. Sci.*, 30, 790–795, doi:10.1007/s00376-012-2187-4,
465 2013.

466 Huffman, G. J., Adler, R. F., Arkin, P., Chang, A., Ferraro, R., Gruber, A., Janowiak, J.,
467 McNab, A., Rudolf, B., and Schneider, U.: The Global Precipitation Climatology
468 Project (GPCP) Combined Precipitation Dataset, *B. Am. Meteorol. Soc.*, 78, 5–
469 20, doi:10.1175/1520-0477(1997)078<0005:TGPCPG>2.0.Co;2, 1997.

470 Ineson, S. and Scaife, A. A.: The role of the stratosphere in the European climate
471 response to El Nino, *Nat. Geosci.*, 2, 32–36, doi:10.1038/NGEO381, 2009.

472 Ivy, D. J., Solomon, S., Calvo, N., and Thompson, D. W.: Observed connections of
473 Arctic stratospheric ozone extremes to Northern Hemisphere surface climate,
474 *Environ. Res. Lett.*, 12, 024004, doi:10.1088/1748-9326/aa57a4, 2017.

475 Kang, S. M., Polvani, L. M., Fyfe, J. C., and Sigmond, M.: Impact of Polar Ozone
476 Depletion on Subtropical Precipitation, *Science*, 332, 951–954,
477 doi:10.1126/science.1202131, 2011.

478 Karpechko, A. Y., Perlwitz, J., and Manzini, E.: A model study of tropospheric
479 impacts of the Arctic ozone depletion 2011, *J. Geophys. Res.*, 119, 7999–8014,
480 doi:10.1002/2013JD021350, 2014.

481 Kidston, J., Scaife, A. A., Hardiman, S. C., Mitchell, D. M., Butchart, N., Baldwin, M.

482 P., and Gray, L. J.: Stratospheric influence on tropospheric jet streams, storm
483 tracks and surface weather, *Nat. Geosci.*, 8, 433–440, doi:10.1038/NGEO2424,
484 2015.

485 Labitzke, K. and Naujokat, B.: The lower Arctic stratosphere in winter since 1952,
486 *Sparc Newsletter*, 15, 11–14, 2000.

487 Lau, K. M., Kim, K. M., and Shen, S. S.: Potential predictability of seasonal
488 precipitation over the U.S. from canonical ensemble correlation
489 predictions, *Geophys. Res. Lett.*, 29, 1–4, doi:10.1029/2001GL014263, 2002.

490 Li, F., Vikhliayev, Y. V., Newman, P. A., Pawson, S., Perlwitz, J., Waugh, D. W., and
491 Douglass, A. R.: Impacts of Interactive Stratospheric Chemistry on Antarctic and
492 Southern Ocean Climate Change in the Goddard Earth Observing System,
493 Version 5 (GEOS-5), *J. Climate*, 29, 3199–3218, doi:10.1175/JCLI-D-15-0572.1,
494 2016.

495 Lu, J., Deser, C., and Reichler, T.: Cause of the widening of the tropical belt since
496 1958, *Geophys. Res. Lett.*, 36, L03803, doi:10.1029/2008GL036076, 2009.

497 Manney, G. L., Santee, M. L., Rex, M., Livesey, N. J., Pitts, M. C., Veefkind, P., Nash,
498 E. R., Wohltmann, I., Lehmann, R., Froidevaux, L., Poole, L. R., Schoeberl, M.
499 R., Haffner, D. P., Davies, J., Dorokhov, V., Gernandt, H., Johnson, B., Kivi, R.,
500 Kyrö, E., Larsen, N., Levelt, P. F., Makshtas, A., McElroy, C. T., Nakajima, H.,
501 Parrondo, M. C., Tarasick, D. W., von der Gathen, P., Walker, K. A., and
502 Zinoviev, N. S.: Unprecedented Arctic ozone loss in 2011, *Nature*, 478, 469–475,
503 <https://doi.org/10.1038/nature10556>, 2011.

504 Manney, G. L. and Lawrence, Z. D.: The major stratospheric final warming in 2016:
505 dispersal of vortex air and termination of Arctic chemical ozone loss, *Atmos.*
506 *Chem. Phys.*, 16, 15371–15396, doi:10.5194/acp-16-15371-2016, 2016.

507 Marsh, D. R., Mills, M. J., Kinnison, D. E., Lamarque, J. F., Calvo, N., and Polvani, L.
508 M.: Climate Change from 1850 to 2005 Simulated in CESM1(WACCM), *J.*
509 *Climate*, 26, 7372–7391, doi:10.1175/JCLI-D-12-00558.1, 2013.

510 McCormack, J. P., Nathan, T. R., and Cordero, E. C.: The effect of zonally
511 asymmetric ozone heating on the Northern Hemisphere winter polar stratosphere,
512 *Geophys. Res. Lett.*, 38, 1–5, doi: 10.1029/2010GL045937, 2011.

513 McLandress, C., Shepherd, T. G., Scinocca, J. F., Plummer, D. A., Sigmond, M.,
514 Jonsson, A. I., and Reader, M. C.: Separating the dynamical effects of climate
515 change and ozone depletion. Part II: Southern Hemisphere troposphere, *J.*
516 *Climate*, 24, 1850–1868, doi:10.1175/2010JCLI3958.1, 2011.

517 Min, S. K. and Son, S. W.: Multimodel attribution of the Southern Hemisphere
518 Hadley cell widening: Major role of ozone depletion, *J. Geophys. Res.*, 118,
519 3007–3015, doi:10.1002/jgrd.50232, 2013.

520 Namias, J.: Some causes of U.S. drought, *J. Clim. Appl. Meteorol.*, 22, 30–39,
521 doi:10.1175/1520-0450(1983)022<0030:Scousd>2.0.Co;2, 1983.

522 Neale, R. B., Richter, J., Park, S., Lauritzen, P. H., Vavrus, S. J., Rasch, P. J., and
523 Zhang, M. H.: The Mean Climate of the Community Atmosphere Model (CAM4)
524 in Forced SST and Fully Coupled Experiments, *J. Climate*, 26, 5150–5168,
525 doi:10.1175/JCLI-D-12-00236.1, 2013.

526 Nowack, P. J., Abraham, N. L., Maycock, A. C., Braesicke, P., Gregory, J. M., Joshi,
527 M. M., Osprey, A., and Pyle, J. A.: A large ozone-circulation feedback and its
528 implications for global warming assessments, *Nat. Clim. Change*, 5, 41–45,
529 doi:10.1038/NCLIMATE2451, 2015.

530 Nowack, P. J., Braesicke, P., Abraham, N. L., and Pyle, J. A.: On the role of ozone
531 feedback in the ENSO amplitude response under global warming, *Geophys. Res.
532 Lett.*, 44, 3858–3866, doi: 10.1002/2016GL072418, 2017.

533 Nowack, P. J., Abraham, N. L., Braesicke, P., and Pyle, J. A.: The impact of
534 stratospheric ozone feedbacks on climate sensitivity estimates, *J. Geophys. Res.*,
535 123, 4630–4641, doi: 10.1002/2017JD027943, 2018.

536 Pawson, S. and Naujokat, B.: The cold winters of the middle 1990s in the northern
537 lower stratosphere, *J. Geophys. Res.*, 104, 14209–14222,
538 doi:10.1029/1999JD900211, 1999.

539 Polvani, L. M., Waugh, D. W., Correa, G. J., and Son, S.-W.: Stratospheric ozone
540 depletion: The main driver of twentieth-century atmospheric circulation changes
541 in the Southern Hemisphere, *J. Climate*, 24, 795–812,
542 doi:10.1175/2010JCLI3772.1, 2011.

543 Ramaswamy, V., Schwarzkopf, M. D., and Randel, W. J.: Fingerprint of ozone
544 depletion in the spatial and temporal pattern of recent lower-stratospheric cooling,
545 *Nature*, 382, 616–618, doi:10.1038/382616a0, 1996.

546 Randel, W. J.: The Seasonal Evolution of Planetary-Waves in the
547 Southern-Hemisphere Stratosphere and Troposphere, *Quarterly Journal of the*

548 Royal Meteorological Society, 114, 1385–1409, doi:10.1002/qj.49711448403,
549 1988.

550 Randel, W. J. and Wu, F.: Cooling of the arctic and antarctic polar stratospheres due to
551 ozone depletion, *J. Climate*, 12, 1467–1479,
552 doi:10.1175/1520-0442(1999)012<1467:COTAAA>2.0.Co;2, 1999.

553 Randel, W. J. and Wu, F.: A stratospheric ozone profile data set for 1979-2005:
554 Variability, trends, and comparisons with column ozone data, *J. Geophys. Res.*,
555 112, D06313, doi:10.1029/2006JD007339, 2007.

556 Ravishankara, A. R., Turnipseed, A. A., Jensen, N. R., Barone, S., Mills, M., Howard,
557 C. J., and Solomon, S.: Do hydrofluorocarbons destroy stratospheric ozone?,
558 *Science*, 263, 71–75, doi:10.1126/science.263.5143.71, 1994.

559 Ravishankara, A. R., Daniel, J. S., and Portmann, R. W.: Nitrous oxide (N₂O): the
560 dominant ozone-depleting substance emitted in the 21st century, *Science*, 326,
561 123–125, doi:10.1126/science.1176985, 2009.

562 Reichler, T., Kim, J., Manzini, E., and Kroger, J.: A stratospheric connection to
563 Atlantic climate variability, *Nat. Geosci.*, 5, 783–787, doi:10.1038/NGEO1586,
564 2012.

565 Russell, J. L., Dixon, K. W., Gnanadesikan, A., Stouffer, R. J., and Toggweiler, J. R.:
566 The Southern Hemisphere westerlies in a warming world: Propping open the
567 door to the deep ocean, *J. Climate*, 19, 6382–6390, doi:10.1175/JCLI3984.1,
568 2006.

569 Smith, K. L. and Polvani, L. M.: The surface impacts of Arctic stratospheric ozone

570 anomalies, *Environ. Res. Lett.*, 9, 074015, doi:10.1088/1748-9326/9/7/074015,
571 2014.

572 Solomon, S.: Antarctic ozone: Progress towards a quantitative understanding, *Nature*,
573 347, 354, doi:10.1038/347347a0, 1990.

574 Solomon, S.: Stratospheric ozone depletion: A review of concepts and history, *Rev.*
575 *Geophys.*, 37, 275–316, doi:10.1029/1999RG900008, 1999.

576 Son, S.-W., Tandon, N. F., Polvani, L. M., and Waugh, D. W.: Ozone hole and
577 Southern Hemisphere climate change, *Geophys. Res. Lett.*, 36, L15705,
578 doi:10.1029/2009GL038671, 2009.

579 Son, S.-W., Gerber, E. P., Perlwitz, J., Polvani, L. M., Gillett, N. P., Seo, K.-H., Eyring,
580 V., Shepherd, T. G., Waugh, D., Akiyoshi, H., Austin, J., Baumgaertner, A.,
581 Bekki, S., Braesicke, P., Brühl, C., Butchart, N., Chipperfield, M. P., Cugnet, D.,
582 Dameris, M., Dhomse, S., Frith, S., Garny, H., Garcia, R., Hardiman, S. C.,
583 Jöckel, P., Lamarque, J. F., Mancini, E., Marchand, M., Michou, M., Nakamura,
584 T., Morgenstern, O., Pitari, G., Plummer, D. A., Pyle, J., Rozanov, E., Scinocca, J.
585 F., Shibata, K., Smale, D., Teyssède, H., Tian, W., and Yamashita, Y.: Impact of
586 stratospheric ozone on Southern Hemisphere circulation change: A multimodel
587 assessment, *J. Geophys. Res.*, 115, D00M07, doi.org/10.1029/2010JD014271,
588 2010.

589 Thompson, D. W. J. and Solomon, S.: Interpretation of recent Southern Hemisphere
590 climate change, *Science*, 296, 895–899, doi:10.1126/science.1069270, 2002.

591 Thompson, D. W. J., Solomon, S., Kushner, P. J., England, M. H., Grise, K. M., and

592 Karoly, D. J.: Signatures of the Antarctic ozone hole in Southern Hemisphere
593 surface climate change, *Nature Geosci.*, 4, 741–749, doi:10.1038/NGEO1296,
594 2011.

595 Ting, M. and Wang, H.: Summertime US Precipitation Variability and Its Relation
596 to Pacific Sea Surface Temperature, *J. Climate*, 10, 1853–1873,
597 doi:10.1175/1520-0442(1997)010<1853:SUSPVA>2.0.CO;2, 1997.

598 Tung, K. K.: On the Relationship between the Thermal Structure of the Stratosphere
599 and the Seasonal Distribution of Ozone, *Geophys. Res. Lett.*, 13, 1308–1311,
600 doi:10.1029/GL013i012p01308, 1986.

601 Wang, F., Yang, S., Higgins, W., Li, Q. P., and Zuo, Z. Y.: Long-term changes in total
602 and extreme precipitation over China and the U.S. and their links to
603 oceanic-atmospheric features, *Int. J. Climatol.*, 34, 286–302,
604 doi:10.1002/joc.3685, 2014.

605 Wang, H. and Ting, M. F.: Covariabilities of winter US precipitation and Pacific Sea
606 surface temperatures, *J. Climate*, 13, 3711–3719,
607 doi:10.1175/1520-0442(2000)013<3711:Cowusp>2.0.Co;2, 2000.

608 Wang, L., Ting, M., Kushner, P. J.: A robust empirical seasonal prediction of winter
609 NAO and surface climate, *Sci. Rep.*, 7, 279, 2017.

610 Waugh, D. W., Garfinkel, C. I., and Polvani, L. M.: Drivers of the Recent Tropical
611 Expansion in the Southern Hemisphere: Changing SSTs or Ozone Depletion?, *J.*
612 *Climate*, 28, 6581–6586, doi:10.1175/JCLI-D-15-0138.1, 2015.

613 WMO: Scientific Assessment of Ozone depletion: 2002. In: *Global Ozone Research*

614 and Monitoring Project, Report No. 47, Geneva, 498 pp., 2003.

615 WMO: Scientific Assessment of Ozone Depletion: 2010. WMO Tech. Note 52, World
616 Meteorological Organization, Geneva, Switzerland, 516 pp., 2011.

617 Xie, F., Li, J., Tian, W., Fu, Q., Jin, F.-F., Hu, Y., Zhang, J., Wang, W., Sun, C., Feng,
618 J., Yang, Y., and Ding, R.: A connection from Arctic stratospheric ozone to El
619 Niño-Southern Oscillation, *Environ. Res. Lett.*, 11, 124026,
620 doi:10.1088/1748-9326/11/12/124026, 2016.

621 Xie, F., Li, J., Zhang, J., Tian, W., Hu, Y., Zhao, S., Sun, C., Ding, R., Feng, J., Yang,
622 Y.: Variations in North Pacific sea surface temperature caused by Arctic
623 stratospheric ozone anomalies, *Environ. Res. Lett.*, 12, 114023,
624 doi:10.1088/1748-9326/aa9005, 2017a.

625 Xie, F., Zhang, J., Sang, W., Li, Y., Qi, Y., Sun, C., and Shu, J.: Delayed effect of
626 Arctic stratospheric ozone on tropical rainfall, *Atmos. Sci. Lett.*, 18, 409–416,
627 2017b.

628 Xie, F., Ma, X., Li, J., Huang, J., Tian, W., Zhang, J., Hu, Y., Sun, C., Zhou, X., Feng,
629 J., Yang, Y.: An advanced impact of Arctic stratospheric ozone changes on spring
630 precipitation in China, *Clim. Dyn.*, <https://doi.org/10.1007/s00382-018-4402-1>,
631 2018.

632 Yin, J. H.: A consistent poleward shift of the storm tracks in simulations of 21st
633 century climate, *Geophys. Res. Lett.*, 32, L18701, doi:10.1029/2005GL023684,
634 2005.

635 Zhang, J. K., Tian, W. S., Chipperfield, M. P., Xie, F., and Huang, J. L.: Persistent

636 shift of the Arctic polar vortex towards the Eurasian continent in recent decades,
637 Nat. Clim. Change., 6, 1094–1099, doi:10.1038/nclimate3136, 2016.

638 Zhang J. K., Tian, W. S., Xie, F., Chipperfield, M. P., Feng, W. H., Son, S-W.,
639 Abraham, N. L., Archibald, A. T., Bekki, S., Butchart, N., Deushi, M., Dhomse,
640 S., Han, Y. Y., Jöckel, P., Kinnison, D., Kirner, O., Michou, M., Morgenstern, O.,
641 O’Connor, F. M., Pitari, G., Plummer, D. A., Revell, L. E., Rozanov, E., Visionsi,
642 D., Wang, W. K., Zeng, G.: Stratospheric ozone loss over the Eurasian continent
643 induced by the polar vortex shift, Nat. Commun., 9, 206,
644 doi.org/10.1038/s41467-017-02565-2, 2018.

645 **Table 1.** CESM-WACCM4 experiments with various specified ozone and SST
 646 forcing.

Exp ^{*1}	Specified ozone and SST forcing	Other forcing
R1	Time-slice run as the control experiment used case F_2000_WACCM_SC. The specified ozone forcing is a 12-month cycle of monthly ozone averaged from 1995 to 2005. The specified SST forcing is a 12-month cycle of monthly SST averaged from 1995 to 2005.	Fixed solar constant, fixed greenhouse gas (GHG) values (averages of emissions scenario A2 of the Intergovernmental Panel on Climate Change (WMO, 2003) over the period 1995–2005), volcanic aerosols (from the Stratospheric Processes and their Role in Climate (SPARC) Chemistry–Climate Model Validation (CCMVal) REF-B2 scenario recommendations), and QBO phase signals with a 28-month zonal wind fixed cycle.
R2	Same as R1, except that the March ozone in the region 30°–90°N at 300–30 hPa ^{*2} is decreased by 15% compared with R1.	Same as R1
R3	Same as R1, except that March ozone in the region 30°–90°N at 300–30 hPa is increased by 15% compared with R1.	Same as R1
R4	Same as R2, except that SST anomalies in the region 0°–70°N and 120°E–90°W related to negative ASO anomalies ^{*3} is added in the SST forcing in April.	Same as R1
R5	Same as R3, except that SST anomalies in the region 0°–70°N and 120°E–90°W related to positive ASO anomalies ^{*4} is added in the SST forcing in April.	Same as R1
R6	Same as R1, except that SST anomalies in the region 0°–70°N and 120°E–90°W related to negative ASO anomalies ^{*3} is added in the SST forcing in April.	Same as R1

R7 Same as R1, except that SST anomalies in the region 0°–70°N and 120°E–90°W related to positive ASO anomalies^{*4} is added in the SST forcing in April. Same as R1

647 ^{*1}Integration time for time-slice runs is 33 years.

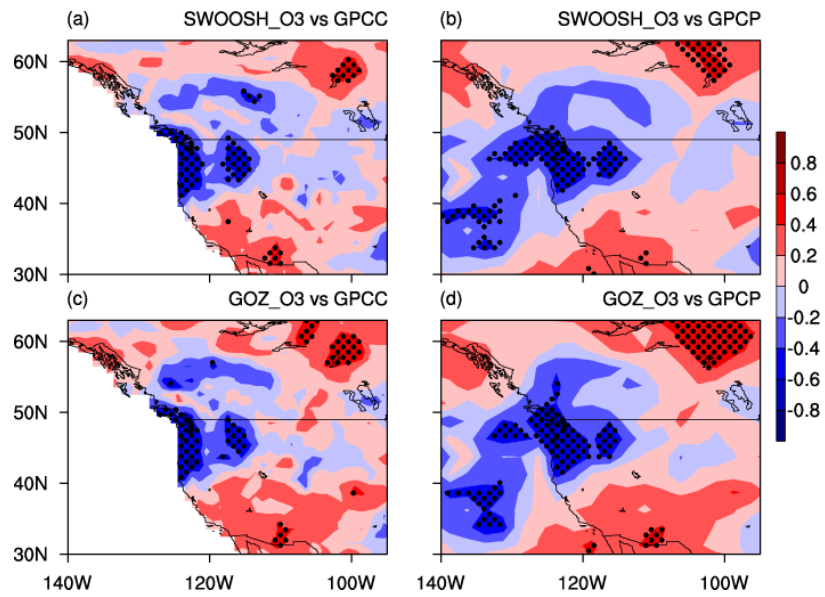
648 ^{*2}To avoid the effect of the boundary of ozone change on the Arctic stratospheric
649 circulation simulation, the replaced region (30°–90°N, 300–30 hPa) was larger than
650 the region used to define the ASO index (60°–90°N, 100–50 hPa).

651 ^{*3}For SST anomalies, see Fig. 9a.

652 ^{*4}For SST anomalies, see Fig. 9b.

653 **Table 2.** Selected positive and negative years for March ASO anomaly events based
 654 on SWOOSH data for the period 1984–2016. Positive and negative March ASO
 655 anomaly events are defined using a normalized time series of March ASO variations
 656 from 1984 to 2016. Values larger than 1 standard deviation are defined as positive
 657 March ASO anomaly events, and those below -1 standard deviation are defined as
 658 negative March ASO anomaly events.

Positive March ASO anomaly events	Negative March ASO anomaly events
1998, 1999, 2001, 2004, 2010	1993, 1995, 1996, 2000, 2011



659

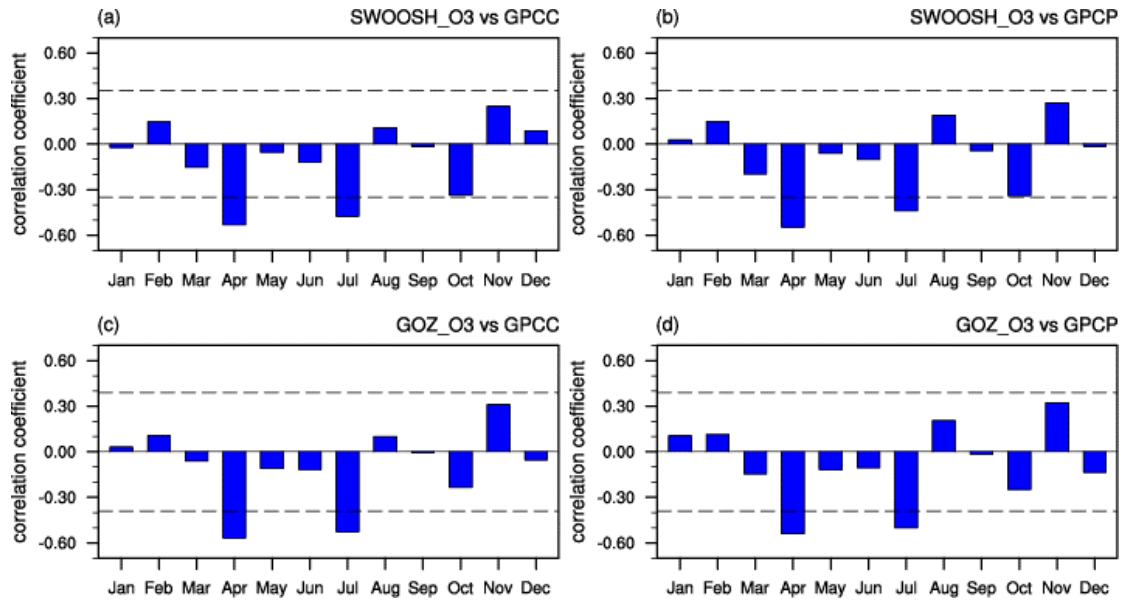
660 **Figure 1.** Correlation coefficients between March ASO and April precipitation

661 variations calculated from SWOOSH (a, b) and GOZCARDS (c, d) ozone, and GPCP

662 (a, c) and GPCP (b, d) rainfall for the period 1984–2016. Dots denote significance at

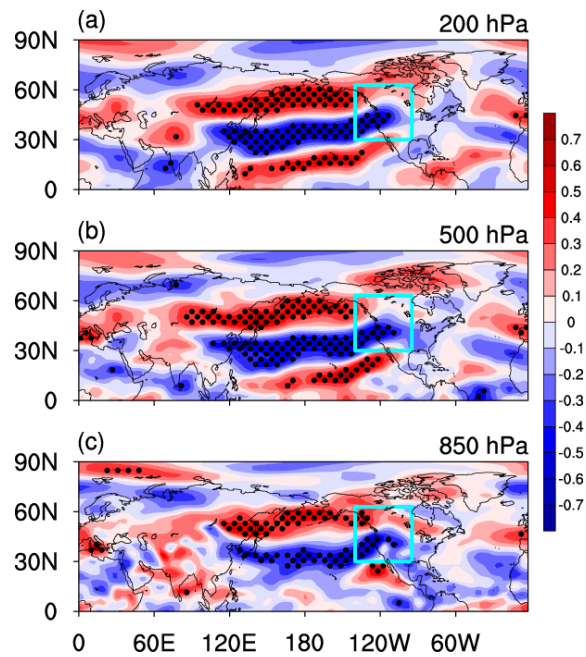
663 the 95% confidence level, according to Student’s t-test. The long-term linear trend

664 and seasonal cycle in all variables were removed before the correlation analysis.



665

666 **Figure 2.** (a) Correlation coefficients between March ASO index and precipitation
 667 anomalies in the northwestern US (43° – 50° N, 115° – 130° W) for each month
 668 calculated from SWOOSH (a, b) and GOZCARDS (c, d) ozone, and GPCC (a, c) and
 669 GPCP (b, d) rainfall for the period 1984–2016. The dashed blacked lines refer to the
 670 correlation coefficient that is significance at 95% confidence level. The long-term
 671 linear trend and seasonal cycle were removed from the original datasets before
 672 calculating the correlation coefficients.



673

674 **Figure 3.** Correlation coefficients between March ASO index and April zonal wind

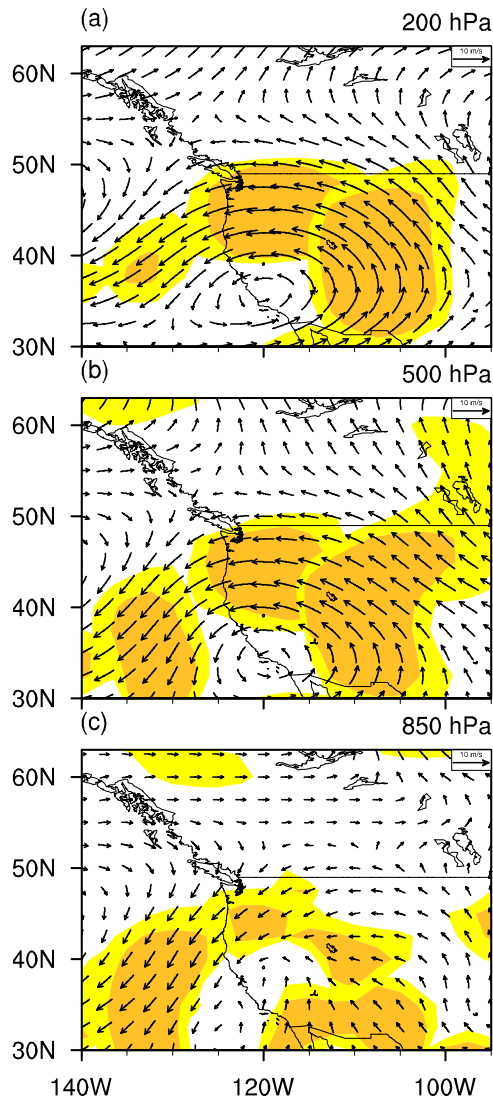
675 variations (m/s, from NCEP2) from 1984 to 2016 at 200 hPa (a), 500 hPa (b), and 850

676 hPa (c). Dots denote significance at the 95% confidence level, according to Student's

677 *t*-test. Blue square is the area shown in Fig. 1. Before performing the analysis, the

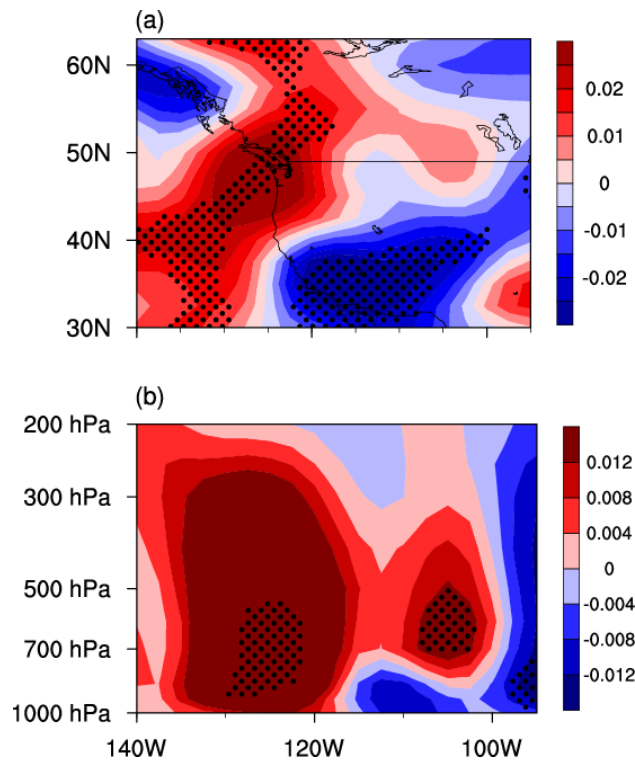
678 seasonal cycle and linear trend were removed from the original datasets. ASO data is

679 from SWOOSH.



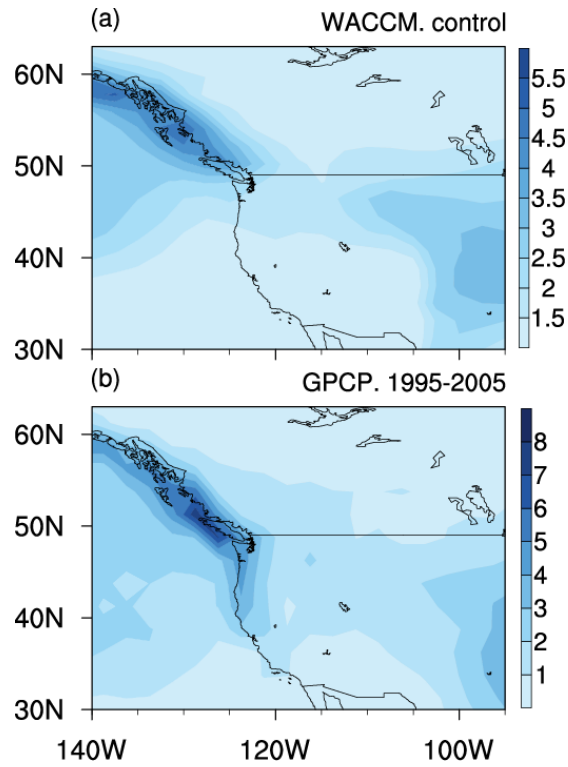
680

681 **Figure 4.** Differences in composite April winds (vectors, m/s, from NCEP2) between
 682 positive and negative ASO anomaly events at 200 hPa (a), 500 hPa (b), and 850 hPa
 683 (c) for 1984–2016. Colored regions are statistically significant at the 90% (light
 684 yellow) and 95% (dark yellow) confidence levels. The seasonal cycle and linear trend
 685 were removed from the original dataset. The ASO anomaly events are selected based
 686 on Table 2.



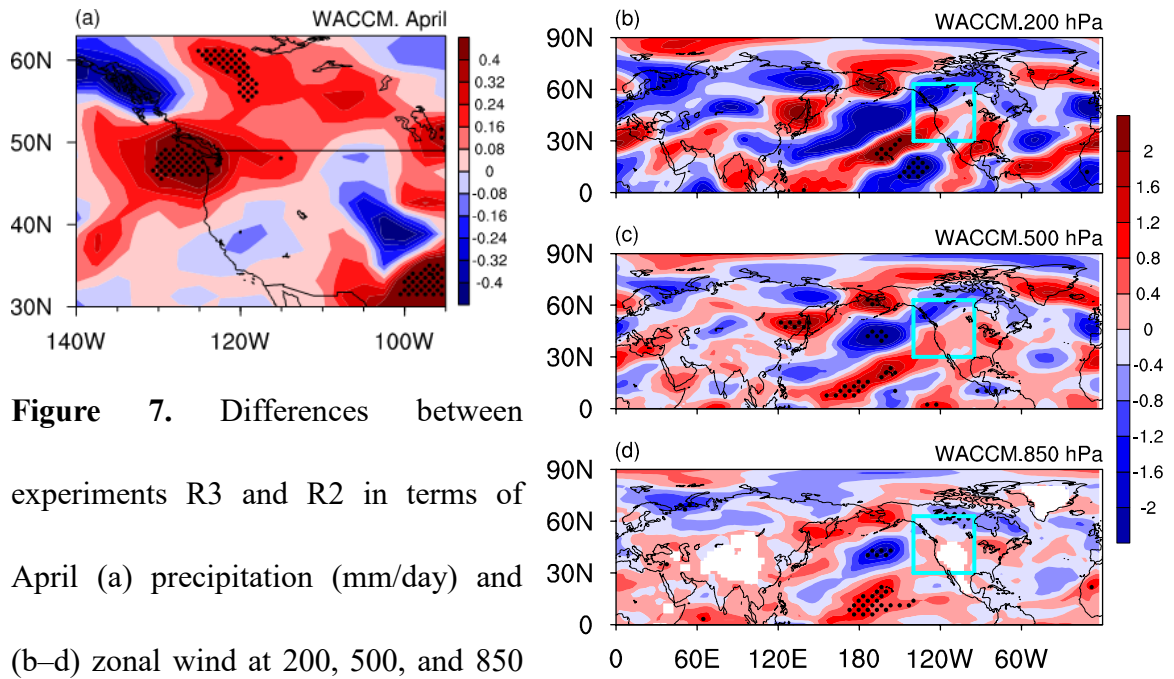
687

688 **Figure 5.** (a) Longitude–latitude cross-section of differences in composite April
 689 vertical velocity anomalies (averaged over 1000–500 hPa) between positive and
 690 negative ASO anomaly events for 1984–2016. (b) Longitude–height cross-section of
 691 differences in composite April vertical velocity anomalies (averaged over 43°–50°N)
 692 between positive and negative ASO anomaly events from 1984 to 2016. Blue is
 693 upward motion and red is downward motion. Dots denote significance at the 95%
 694 confidence level. Before performing the analysis, the seasonal cycle and linear trend
 695 were removed from the original dataset. The ASO anomaly events are selected based
 696 on Table 2. The vertical velocity (Pa/s) dataset is from NCEP2.



697

698 **Figure 6.** (a) Spatial distribution of April precipitation (mm/day) climatology in the
 699 control experiment (R1). (b) Same as (a), but precipitation from the GPCP for the
 700 period 1995–2005. For details of specific experiments, see Table 1.



701

702

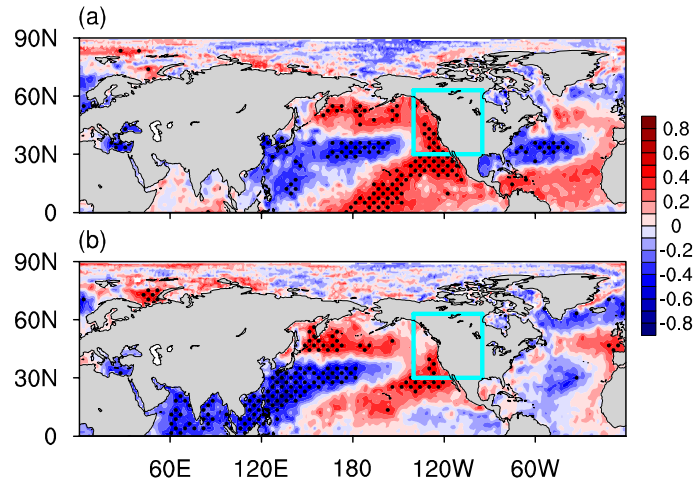
703

704

705

706

Figure 7. Differences between experiments R3 and R2 in terms of April (a) precipitation (mm/day) and (b–d) zonal wind at 200, 500, and 850 hPa, respectively. Dots denote significance at the 95% confidence level.



707

708 **Figure 8.** (a) Correlation coefficients between regional precipitation (43° – 50° N,

709 115° – 130° W) and SST variations in April for 1984–2016. (b) Correlation coefficients

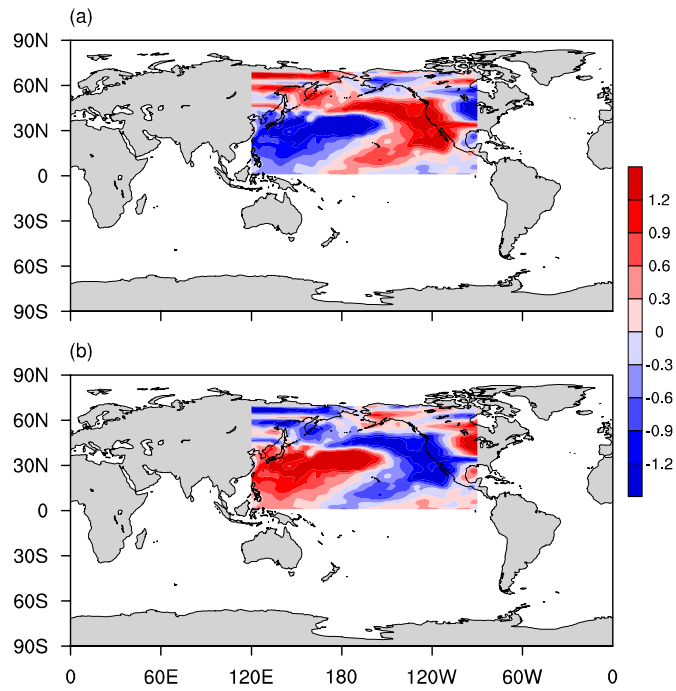
710 between March ASO ($\times -1$) and April SST variations for 1984–2016. Dots denote

711 significance at the 95% confidence level, according to Student's *t*-test. Before

712 performing the analysis, the seasonal cycle and linear trend were removed from the

713 original data. ASO data is from SWOOSH, precipitation from GPCP, and SST from

714 HadSST.



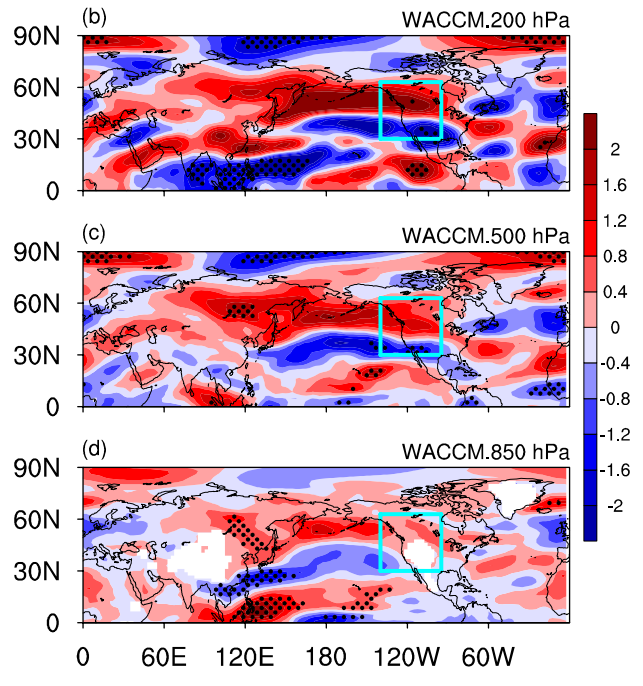
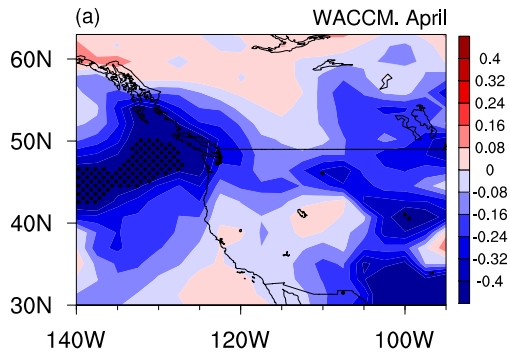
715

716 **Figure 9.** (a) Composite SST anomalies during negative ASO anomaly events. (b)

717 Composite SST anomalies during positive ASO anomaly events. The ASO anomaly

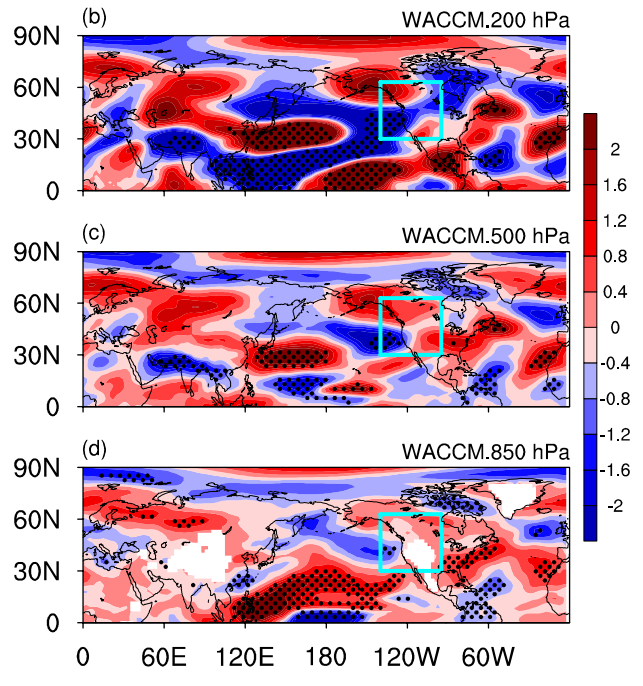
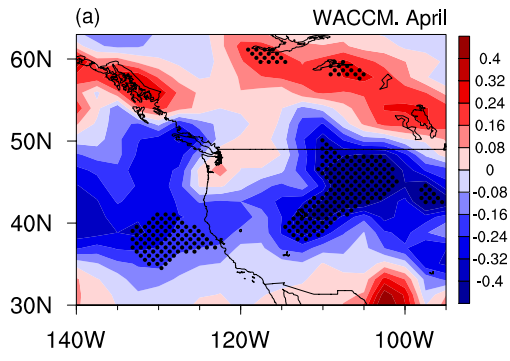
718 events are selected based on Table 2. SST data is from CESM SST forcing data.

719



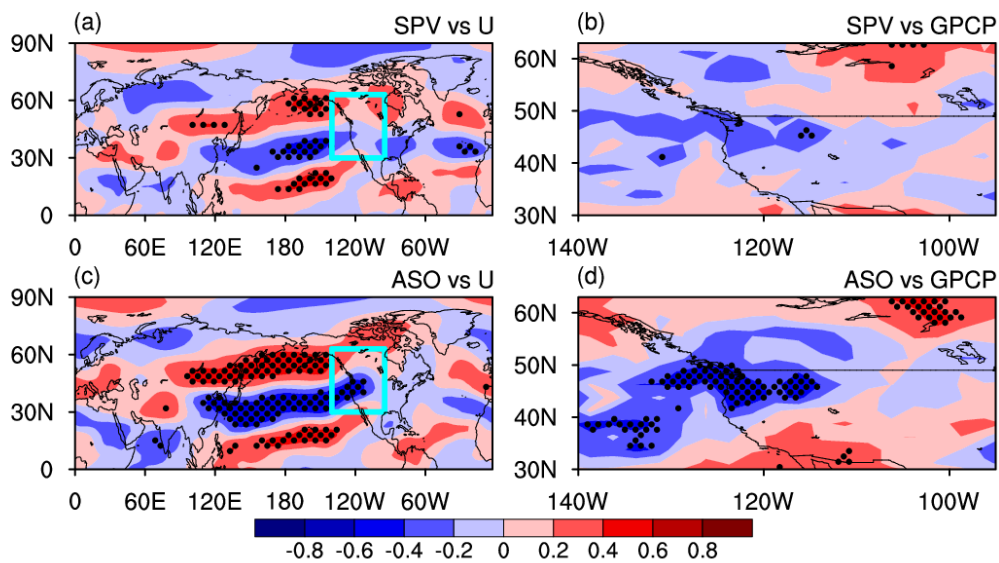
720

721 **Figure 10.** Same as Fig. 7, but for the
 722 difference between experiments R5 and
 723 R4.
 724



725
726
727
728
729
730
731

Figure 11. Same as Fig. 7, but for the difference between experiments R7 and R6.



732

733 **Figure 12.** (a) Correlation coefficients between the February $-SPV$ ($10^5 \text{ K m}^2 \text{ kg}^{-1} \text{ s}^{-1}$)
 734 index defined by Zhang et al. (2018) and April zonal wind variations at 200 hPa for
 735 1984–2016. (b) Correlation coefficients between February $-SPV$ index and April
 736 precipitation variations. (c) and (d) As for (a) and (b), but between March ASO and
 737 April 200 hPa zonal wind and April precipitation variations. Dots denote significance
 738 at the 95% confidence level, according to Student’s t -test. The long-term linear trend
 739 and seasonal cycle in all variables were removed before the correlation analysis. The
 740 ASO data is from SWOOSH, zonal wind from NCEP2, and precipitation from GPCP.